Nat. Hazards Earth Syst. Sci., 22, 3413–3433, 2022
https://doi.org/10.5194/nhess-22-3413-2022

Natural Hazards and Earth System Sciences
Open Access
EGU

Wind-wave characteristics and extremes along the Emilia-Romagna coast

Umesh Pranavam Ayyappan Pillai[1], Nadia Pinardi[1], Ivan Federico[2], Salvatore Causio[2], Francesco Trotta[1], Silvia Unguendoli[3], and Andrea Valentini[3]

[1]Department of Physics and Astronomy, University of Bologna, Bologna, 40127, Italy
[2]Euro-Mediterranean Center on Climate Change, Lecce, 73100, Italy
[3]Hydro-Meteo-Climate Service of the Agency for Prevention, Environment and Energy of Emilia-Romagna, Arpae-SIMC, Bologna, 40122, Italy

Correspondence: Umesh Pranavam Ayyappan Pillai (umesh.pranavam@unibo.it)

Received: 22 March 2022 – Discussion started: 4 April 2022
Revised: 23 July 2022 – Accepted: 17 September 2022 – Published: 19 October 2022

Abstract. This study examines the wind-wave characteristics along the Emilia-Romagna coasts (northern Adriatic Sea, Italy) with a 10-year wave simulation for the period 2010–2019 performed with the high-resolution unstructured-grid WAVEWATCH III (WW3) coastal wave model. The wave parameters (significant wave height, mean and peak wave period, and wave direction) were validated with the in situ measurements at a coastal station, Cesenatico. In the coastal belt, the annual mean wave heights varied from 0.2–0.4 m, and the seasonal mean was highest for the winter period (> 0.4 m). The Emilia-Romagna coastal belt was characterized by wave and spectra seasonal signals with two dominant frequencies of the order of 10 and 5–6 s for autumn and winter and 7–9 and 4 s for spring and summer. The wavelet power spectra of significant wave height for 10 years show considerable variability, having monthly and seasonal periods. This validated and calibrated data set enabled us to study the probability distributions of the significant wave height along the coasts and define a hazard index based on a fitted Weibull probability distribution function.

1 Introduction

The wind-induced stress on the sea surface gives rise to wind waves that affect human activities on the coasts (Armaroli et al., 2019). The prevailing wind waves of a region determine the defence performance of coastal and offshore structures, and therefore precise information on wind waves is crucial for coastal operations and defence systems. During extreme events, the wind waves modify the total water-level elevation, leading to a higher risk of overtopping which can damage infrastructures. The Intergovernmental Panel on Climate Change (IPCC, 2007) has also highlighted the need for a long-term evaluation of wind-wave climate trends for coastal resilience (Hemer et al., 2012). The IPCC (2021) indicates the necessity of a regional evaluation of climate change, with various target factors that can aid in risk management and policy-making. The report points out that over the 21st century, nearshore regions will encounter sea level rise, thereby adding to more persistent coastal flooding (across low-lying regions) and associated coastal erosion.

Across the globe, wave climatology studies using reanalysis data sets and model hindcasts have been reported by Carter et al. (1991), Sterl et al. (1998), Young (1999), Cox and Swail (2001), Sterl and Caires (2005), Hemer et al. (2010), Semedo et al. (2011), Young et al. (2011), Zheng et al. (2016), and De Leo et al. (2020). Wind speed and wave height climatologies with emphasis on the Southern Ocean are described in the works of Young (1999), Young and Holland (1996), and Young and Donelan (2018). Past studies on regional scales (Young et al., 2020) based on observations and numerical modelling have also been reported by various researchers on different regions such as the Northern Hemisphere (Woolf et al., 2002; Reistad et al., 2011), the Southern Hemisphere (Gorman et al., 2003), the Mediterranean Sea (Lionello and Sanna, 2005; Lionello, 2012; Clementi et al., 2017; Ravdas et al., 2018; Morales-Márquez et al., 2020;

De Leo et al., 2021; Barbariol et al., 2021; Amarouche et al., 2022), the Persian Gulf (Kamranzad et al., 2013), western Australia (Bosserelle et al., 2012), the eastern North Atlantic (Dodet et al., 2010), the southeast Pacific Ocean (Aguirre et al., 2017), the Indian Ocean (Stopa and Cheung, 2014), the Black Sea (Akpinar and Komurcu, 2013; Arkhipkin et al., 2014; Fedor and Stanislav, 2020), and the China seas (Zheng and Li, 2015; Qian et al., 2020).

Numerous studies have been reported for the Adriatic Sea, using numerical models to demonstrate the wind-wave climate characteristics. In the Adriatic there are many wind-wave forecast systems, including the Henetus forecast system described in Bertotti et al. (2011). Other state-of-the-art models include the Nettuno system as reported in Bertotti et al. (2013), which combines the atmospheric model COSMO (Steppeler et al., 2003) and the wave model WAM (Komen et al., 1994), and SWAN-MEDITARE, which combines COSMO with SWAN (Valentini et al., 2007; Russo et al., 2013). Donatini et al. (2015) have also implemented high-resolution model chains for wind-wave forecasting in the Mediterranean and Adriatic seas, which use a combination of the atmospheric model WRF and wave model MIKE 21 (DHI, 2017). In a study over the Gulf of Taranto in southern Italy, a multi-nesting approach was adopted to evaluate coastal wave dynamics and hydrodynamics (Gaeta et al., 2016). In the Adriatic Sea, Sikiric et al. (2018) implemented the unstructured grid WAVEWATCH III (WW3) (WW3DG, 2016) with 2 km wind forcings from ALADIN forecasts (Farda et al., 2007). The study showed a good match with satellite measurements (SARAL) as compared to CryoSat-2 and Jason-2. The results were in agreement with the studies by Sepulveda et al. (2015), which showed that SARAL estimates of wave heights were far better than CryoSat-2 and Jason-2. Cavaleri et al. (2018) also reported on the application of SARAL data, producing good results.

In a study of the northern Adriatic, Lionello et al. (2012) used the WAM model to predict extreme wind waves and associated storm surge effects. In the Adriatic a modelling combination of WAM + SHYFEM (Komen et al., 1994; Umgiesser et al., 2014) forced with analysis and forecast ECMWF winds was used to forecast the 29 October 2018 storm (Cavaleri et al., 2019) conditions in northern Italy. The application of corrected forecast winds (ECMWF) within these models provided consistent results in line with measurements. High waves in the northern Adriatic Sea were reported in a recent study by Cavaleri et al. (2021).

Studies by Katalinić et al. (2015) reported that in the Adriatic basin, the wind speed and wave height increase from the northern to the southern areas with a maximum mean (annual) H_s of 0.68 m. These results are underestimated as compared with the findings of Queffeulou and Bentamy (2007) resulting from a 14-year (1992–2005) satellite mission that revealed a mean H_s of 0.85 m. Queffeulou and Bentamy (2007) also showed that in the Adriatic Sea, 80 % of the H_s values were lower than 1.10 m. An intercomparison of WAM and WW3 models in the Adriatic and North Sea, based on testing various input physics, was reported by Benetazzo et al. (2021). The analysis aided in investigating the processes that lead to the generation of higher waves in the context of storms.

In the light of several hazardous and extreme events in the Emilia-Romagna (ER) coastal area, several studies have investigated the following: (i) coastal risk and vulnerability to flooding and erosion (Armaroli et al., 2009, 2019; Sekovski et al., 2015; Armaroli and Duo, 2018; Sanuy et al., 2018; Ferrarin et al., 2020); (ii) sea level rise, land subsidence, and littoral hydrodynamics (Perini et al., 2017; Gaeta et al., 2018); (iii) identification of storm thresholds (Armaroli et al., 2012); and (iv) forecasting of coastal flooding (Biolchi et al., 2021, 2022).

To the best of our knowledge, no studies have been carried out to date on the wind and wave characteristics and extremes in the ER coastal belt with high-resolution wind-wave models. Our study focusses on the prevailing wind-wave climatology in the coastal belt of the ER (northern Adriatic Sea) for a period of 10 years (2010–2019), the characterization of the wind-wave regimes, and the study of extreme wave conditions along the coastal belt to quantitatively determine the extreme wave hazard. We use a specific probability distribution function fitting procedure with the wind-wave model data and thereby extract hazard indices for different coastal points. We believe that our 10-year model simulation with appropriate validation at a coastal location will be useful for hazard estimations along the ER coastal area. For the first time we discuss the probability distribution of waves that are essential to quantify the extremes and their hazard.

The paper is organized as follows. Section 2 outlines the study area. Section 3 describes the wind-wave model used in the study, the model forcing, and the validation buoy data used. Section 4 describes the wind and wave climate in the ER coastal belt together with the wave spectra characteristics and wavelet analysis. Section 5 presents the analysis of the probability density distribution and the hazard index for extreme events. Finally, Sect. 6 summarizes the key findings from the study with a brief conclusion.

2 The study area – the Emilia-Romagna coast

The study area is the coastal waters of Emilia-Romagna, situated in northern Italy along the Adriatic Sea, with a coastline including natural zones and dunes to long stretches sheltered by groynes and breakwaters (Armaroli et al., 2012). The coastline is 130 km long (Harley et al., 2016) with the Po Delta as the northern boundary and the town of Riccione at the southernmost point. Figure 1 shows the study area in the ER coastal belt.

There are two main wind patterns in this region – the bora and sirocco winds (Pandzic and Likso, 2005; Umgiesser et al., 2021). Severe wind storms occur from the east-northeast,

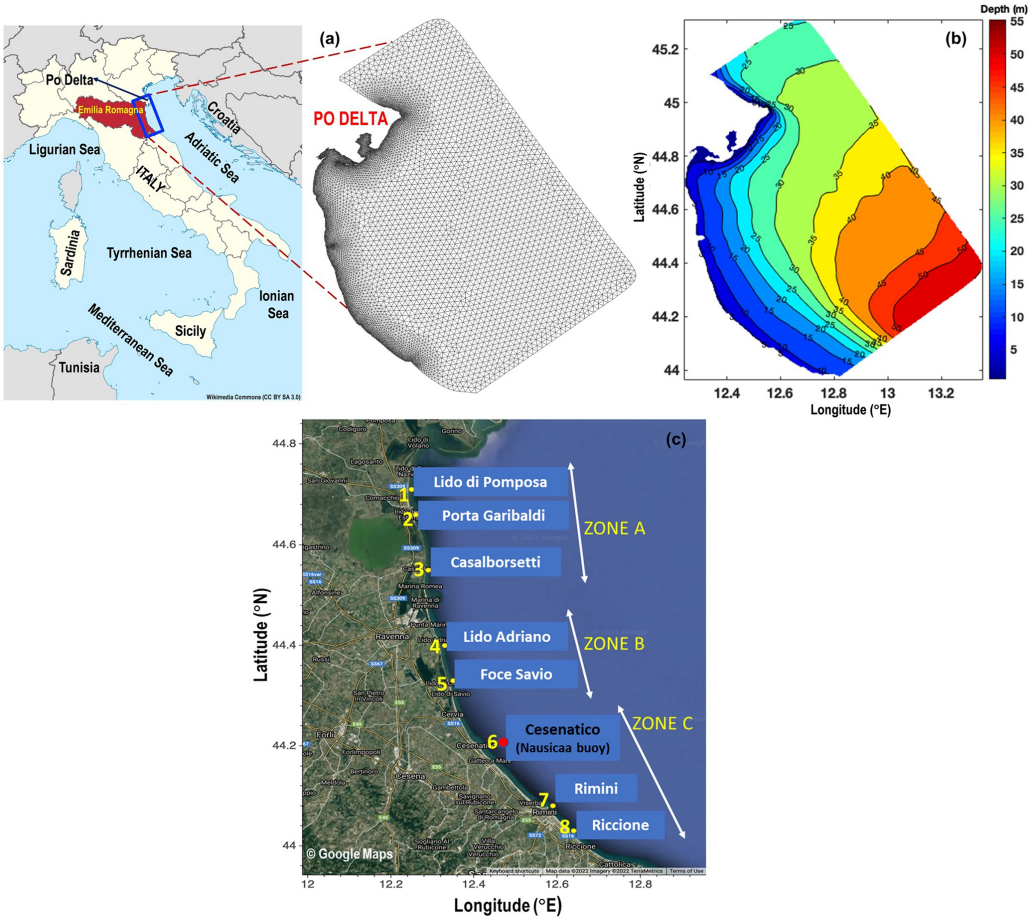

Figure 1. **(a)** The Emilia-Romagna coastal belt with the unstructured mesh, **(b)** bathymetry for the model domain, and **(c)** the control points across the coastal belt used for analysis and validation. The Nausicaa buoy in Cesenatico (at station 6) was used in this study to validate the hindcast wave parameters.

i.e. the prevailing direction of the bora winds. The sirocco winds are associated with low-pressure systems over the Italian Peninsula and the Ionian Sea. Owing to the restricted fetch, i.e. limited extension of the wave generation area, the bora winds generate young and steep waves that break frequently (Cavaleri et al., 1991), while the sirocco winds generate longer-fetch waves across the Adriatic Sea (Cavaleri, 2000). Thus the swell seas are controlled by the sirocco winds and the seas are dominated by the bora winds (Bonaldo et al., 2017).

The ER coastal area is subdivided into three major zones (Fig. 1c) which correspond to different coastal trophic conditions (Fiori et al., 2016). The station locations are the land town locations perpendicular to which the environmental agency monitoring transects are carried out monthly and weekly to monitor the marine ecosystem environmental status. Thus, knowing the prevailing winds and waves at these locations could be of importance for the management of this important coastal area.

The prevailing hydrodynamics show that the region is microtidal with spring tides (80–90 cm) and neap tides (30–40 cm), with strong diurnal and semi-diurnal components (Armaroli and Duo, 2018). A low-energy wave climate (IDROSER, 1996; Ciavola et al., 2017) has been reported along the coastal belt of ER, i.e. 60 % $H_s < 1$ m. Armaroli et al. (2012) reported that waves originating from the east correspond to a proportion of 91 % $H_s < 1.25$ m, owing to the controlled fetch.

3 Numerical wave model set-up

In this study, the third-generation unstructured-grid spectral-wave model, WW3 (version 5.16; WW3DG, 2016) was used to evaluate nearshore waves. WW3 is a universally accepted wave model (Tolman et al., 2002) with continuous updates of ocean wave physics. The model is formulated by solving the action-density balance equation:

$$\frac{\partial N}{\partial t} + \frac{1}{\cos\phi}\frac{\partial}{\partial \phi}\dot{\phi} N \cos\theta + \frac{\partial}{\partial \lambda}\dot{\lambda} N + \frac{\partial}{\partial k}\dot{k} N + \frac{\partial}{\partial \theta}\dot{\theta}_g N = \frac{S}{\sigma}. \quad (1)$$

The left-hand side of Eq. (1) denotes the changes in wave action density (i.e. local rate), generation in physical space, shifting of action density (frequency/direction) owing to spatio-temporal changes in depth, and current. λ denotes longitude, φ latitude, θ direction of wave propagation, and k wave number, and σ and t represent the intrinsic angular frequency and time respectively. The source term used in this paper, S in Eq. (1), is the wind input and dissipation source package ST4 (Ardhuin et al., 2010) or ST6 (Zieger et al., 2015; Rogers et al., 2012; Babanin, 2011), the bottom friction JONSWAP (Joint North Sea Wave Project) parameterization (Hasselmann et al., 1973), or SHOWEX (Shoaling Waves Experiment) formulation (Ardhuin et al., 2003) for sandy bottoms. In the section on sensitivity experiments we used a combination of these source terms.

The WW3 model grid (Fig. 1) is divided into 15 392 elements, linked with 8148 nodes, with a resolution of about 300 m at the coast and 2.5 km at the open boundary (Fig. 1a). The merged European Marine Observation and Data Network (EMODnet) data (250 m resolution) and multibeam high-resolution measurements from Arpae (Regional Agency for Prevention, Environment and Energy of Emilia Romagna) serve as the bathymetry of the ER domain (Fig. 1b). The model spectrum is sampled in 24 directions and 30 frequencies (0.0500–0.7932 Hz), with an increment factor of 1.1. The model time steps are set as the (i) maximum global time step, 200 s; (ii) maximum CFL (Courant–Friedrichs–Lewy) time step X–Y, 50 s; (iii) maximum CFL time step k–θ, 50 s; and (iv) minimum source term time step, 10 s. The source term for linear input and wind input uses the parameterization formulated by Cavaleri and Malanotte-Rizzoli (1981) and Donelan et al. (2006). The Generalized Multiple DIA (GMD) was used to simulate the non-linear interactions (Tolman, 2010, 2013, 2014); the dissipation physics were based on Rogers et al. (2012); and the SHOWEX formulations by Ardhuin et al. (2003) were used to simulate the bottom friction. The SHOWEX parameterization is ripple-induced bottom friction, which considers the formation of sand ripples on the bottom. Breaking (depth-induced) is activated using Battjes and Janssen (1978) physics.

The WW3 model is forced every 6 h with the ECMWF analysis winds at 0.125° horizontal resolution. The model winds were validated at three stations, namely Porto Corsini (44.49° N, 12.28° E), Porto Garibaldi (44.67° N, 12.24° E), and Cesenatico Port (44.20° N, 12.40° E) along the ER coastal belt. The wind speed comparison statistics as indicated in Table 1 showed correlations of the order of 0.7, with bias of $-0.2\,\mathrm{m\,s^{-1}}$ indicative of underestimation of wind speed and RMSE of $1.8\,\mathrm{m\,s^{-1}}$. Larger biases of the order of $-0.6\,\mathrm{m\,s^{-1}}$ and correlations as low as 0.5 exist during summer and some autumn seasons.

Table 1. Quality assessment of ECMWF winds with observed wind speeds for selected stations.

	Wind speed ($\mathrm{m\,s^{-1}}$)				
Statistics	Full year	Winter	Spring	Summer	Autumn
Porto Corsini (year 2013)					
R	0.7	0.7	0.7	0.5	0.7
Bias	−0.2	0.2	−0.1	−0.3	−0.4
RMSE	1.8	1.8	1.9	1.6	2
Porto Garibaldi (year 2018)					
R	0.7	0.8	0.7	0.5	0.8
Bias	−0.2	0.2	−0.3	−0.5	0
RMSE	1.8	1.7	1.6	1.9	1.9
Cesenatico Port (year 2015)					
R	0.7	0.8	0.8	0.5	0.6
Bias	−0.2	0	−0.3	−0.6	0.2
RMSE	1.9	1.7	2	1.9	2

R: correlation; RMSE: root mean square error.

The wave lateral boundary values are provided by the Copernicus Marine Environment Monitoring Service (CMEMS) model (https://marine.copernicus.eu/, last access: 20 March 2022; Korres et al., 2021) at a resolution of ∼ 4.5 km hourly. The open boundary nodes are forced via JONSWAP wave spectrum approximation (Yamaguchi, 1984) based on the CMEMS wave parameters (significant wave height, peak period, and mean direction).

3.1 Wave observational data set and validation method

In order to validate the model hindcasts, we used the wave buoy Nausicaa in Cesenatico (44.21° N, 12.47° E; station 6) as shown in Fig. 1c. This station is situated away from the coast of Cesenatico municipality and is supported with a Datawell Directional Waverider (MkIII 70 wave) buoy called Nausicaa (https://www.arpae.it/it/temi-ambientali/mare/dati-e-indicatori/dati-boa-ondametrica, last access: 20 March 2022) which has been maintained by Arpae since 23 May 2007. The location of the buoy is 8 km offshore of Cesenatico, at a depth of approximately 10 m, in a region inaccessible to fishing, navigation, and moorings. Wave data such as height (H_s), period, and the direction of waves every 30 min constituted the basic validation data set for the modelling period from January 2010 to December 2019.

Wave model parameters such as wave height, period, and direction were extracted and analysed for eight control points as shown in Fig. 1c. The details of the control points are described in Table 2. The model-simulated 1D wave spectra are extracted and analysed based on seasons.

Table 2. Details of control points 1 to 8.

Control points	Station name	Long (°E)	Lat (°N)	Depth (m)	Zone
1	Lido di Pomposa	12.25	44.71	5.8	
2	Porto Garibaldi	12.26	44.66	5.1	A
3	Casalborsetti	12.29	44.55	5.0	
4	Lido Adriano	12.33	44.40	7.7	B
5	Foce Savio	12.35	44.33	5.3	
6	Cesenatico	12.47	44.21	10.4	
7.	Rimini	12.59	44.08	8.1	C
8.	Riccione	12.64	44.03	6.2	

The skill of the model to reproduce the observations at the Nausicaa buoy location was assessed by standard statistics, namely the correlation coefficient (R), bias, and root mean square error (RMSE):

$$R = \frac{\sum_{i=1}^{n}\left(P_i - \overline{P}\right)\left(O_i - \overline{O}\right)}{\sqrt{\sum_{i=1}^{n}\left(P_i - \overline{P}\right)^2\left(O_i - \overline{O}\right)^2}}, \quad (2)$$

$$\text{bias} = \frac{1}{n}\sum_{i=1}^{n}(P_i - O_i), \quad (3)$$

$$\text{RMSE} = \sqrt{\frac{1}{n}\sum_{i=1}^{n}(P_i - O_i)^2}, \quad (4)$$

where model estimates are denoted by P, O represents observational data, n indicates number of data points, and the overbar denotes mean values.

3.2 Sensitivity experiments for wave model parameterizations

Three sets of sensitivity experiments using WW3 were executed using a combinations of wave physics:

i. ST4 + JONSWAP (EXP1),

ii. ST4 + SHOWEX (EXP2), and

iii. ST6 + SHOWEX (EXP3),

for the representative months of February (winter) and September (autumn) 2018. The combination of ST6 with JONSWAP is not considered because this bottom friction is not suitable for sandy beaches as EXP1 will show.

The H_s comparison with the Nausicaa buoy is shown in Table 3, which highlights that the best physics is given by EXP3. The mean buoy H_s is 0.92 and 0.38 m for February and September 2018 respectively. The comparison of the mean wave period, T_m (not shown), for the three experiments showed a higher performance using the combination of ST6 + SHOWEX. The sensitivity study produced sufficient confidence in using the ST6+SHOWEX physics for the ER region. This wave physics was thus adopted for the 10-year simulation.

Table 3. Skill scores for the sensitivity experiments.

Experiment	Significant wave height (H_s in m)					
	February 2018			September 2018		
	R	Bias (m)	RMSE (m)	R	Bias (m)	RMSE (m)
EXP1	0.93	−0.12	0.29	0.92	−0.15	0.21
EXP2	0.91	−0.09	0.32	0.90	−0.12	0.18
EXP3	0.94	−0.04	0.26	0.96	−0.09	0.14

R: correlation; RMSE: root mean square error.

3.3 Validation of wave hindcasts

The model outputs, such as significant wave height (H_s), mean wave period (T_m), peak wave period (T_p), and mean wave direction (θ_m), were compared with the buoy observations for the 10-year period 2010–2019. Figure 2 shows the 10-year comparison of H_s, which qualitatively demonstrates that the overall model H_s also followed the buoy values in peak events at the Cesenatico station (station 6 in Fig. 1c). This is a consistency check of model against observations as required for "goodness" indicators in numerical weather predictions (Murphy, 1993). The model also captures the seasonal variations at the coastal location. In general, the lower H_s values are slightly overestimated, while higher H_s values are underestimated.

Table 4 shows the validation statistics for each year. The mean of model/buoy estimates for H_s, T_m, and T_p are 0.40/0.45 m, 3.02/3.23 s, and 4.17/4.36 s respectively. On average the model underestimates the measurements (as seen from the negative bias for most of the years). A high correlation is shown, ranging from 0.81 to 0.93 for 2010–2019, with the highest correlation for 2017. The T_m comparison revealed a lower correlation of the order of 0.72 to 0.81, compared to H_s. The negative bias (−0.371 to −0.018 s) indicated an underestimation of T_m, with a corresponding RMSE of the order of 0.79 to 0.91 s. Similarly, the T_p also showed a lower correlation (0.53 to 0.70) in comparison to H_s and T_m. T_p also showed underestimations as revealed from the bias of the order of −0.382 to 0.151 s, with an RMSE varying from 1.48 to 1.78 s.

Figure 3 represents the observations–model scatter plot of H_s for the period 2010–2019 (Fig. 3a) and the seasonal scatter as shown in Fig. 3b–e for station 6. The dashed red line denotes the best data fit for the comparison. The comparison of H_s for 2010–2019 (Fig. 3a) shows that there is relatively good agreement between model H_s and measurements with a high correlation of 0.90. There is a slight underestimation (bias = −0.05 m), with RMSE = 0.21 m. The seasonal

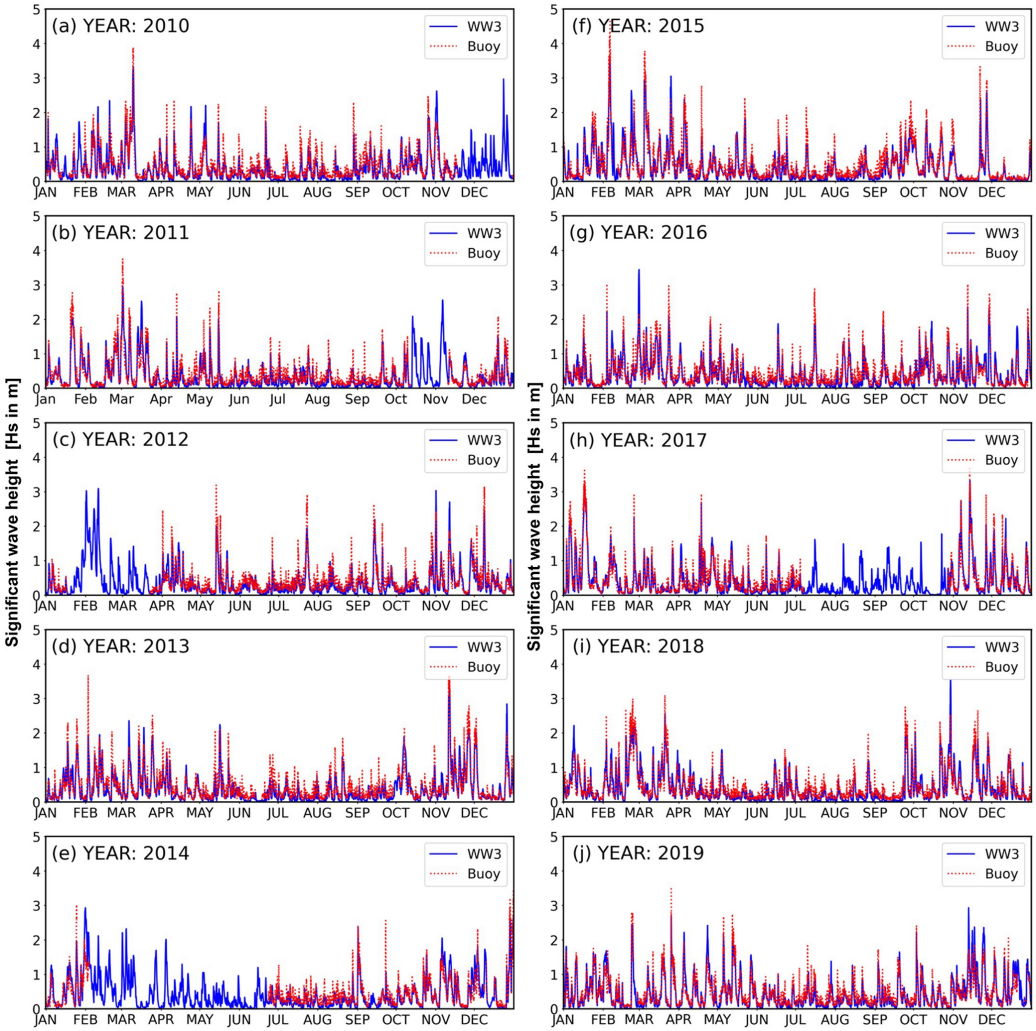

Figure 2. Time series plot of **(a–j)** significant wave height (in metres, indicated by solid blue lines) and observations (dotted red lines) for 2010–2019 at station 6 (Cesenatico; see Fig. 1c for location).

scatters for winter, spring, and autumn (Figs. 3b, c, and e) showed high correlations, with a slight underestimation in relation to buoy observations. The summer seasons (Fig. 3d) showed a comparatively lower correlation with an underestimation of H_s. In general, the model H_s underestimates the buoy data, specifically the higher H_s, and similar underestimations have been reported in many past studies such as Ardhuin et al. (2007), Korres et al. (2011), and Clementi et al. (2017).

The comparison of T_m for 2010–2019 is shown in Fig. 3f and for the seasons in Fig. 3g–j, revealing a larger scatter in comparison to H_s. During 2010–2019 (Fig. 3f), the simulated T_m is lower than the buoy measurements and shows a lower performance ($R = 0.75$) in comparison to H_s. The winter, spring, and autumn seasons (Fig. 3g, h, and j) showed a moderate correlation of 0.74 to 0.75, while the lowest correlation was observed in summer (0.62). For all the seasons, underestimations of T_m were noted, with the maximum in summer ($B = -0.47$ s) and lowest in winter ($B = -0.11$ s).

4 Characterization of the Emilia-Romagna wind and wave fields

4.1 Wind climatology of the Emilia-Romagna coast

Below we present the wind climatology in the ER region based on the ECMWF analysis winds over a period of 10 years. The seasons are presented as winter (December–January–February), spring (March–April–May), summer (June–July–August), and autumn (September–October–November).

Table 4. Statistics of the comparison of buoy measurements (Cesenatico, station 6) with model results for 2010–2019.

Statistics	2010	2011	2012	2013	2014	2015	2016	2017	2018	2019
Significant wave height (H_s in m)										
R	0.882	0.903	0.876	0.814	0.860	0.917	0.890	0.932	0.915	0.897
Bias	−0.055	−0.066	−0.076	−0.065	−0.022	−0.053	−0.045	−0.031	−0.035	−0.016
RMSE	0.211	0.193	0.205	0.211	0.252	0.209	0.201	0.194	0.193	0.206
Mean wave period (T_m in s)										
R	0.718	0.776	0.724	0.739	0.809	0.746	0.740	0.709	0.746	0.777
Bias	−0.23	−0.371	−0.321	−0.255	−0.112	−0.363	−0.194	−0.018	−0.159	−0.071
RMSE	0.911	0.797	0.841	0.872	0.828	0.904	0.804	0.838	0.854	0.821
Peak wave period (T_p in s)										
R	0.653	0.530	0.598	0.621	0.705	0.543	0.603	0.605	0.653	0.642
Bias	−0.305	−0.255	−0.325	−0.273	−0.258	−0.382	−0.183	0.151	−0.084	0.079
RMSE	1.618	1.782	1.611	1.687	1.483	1.860	1.575	1.636	1.597	1.582

R: correlation; RMSE: root mean square error.

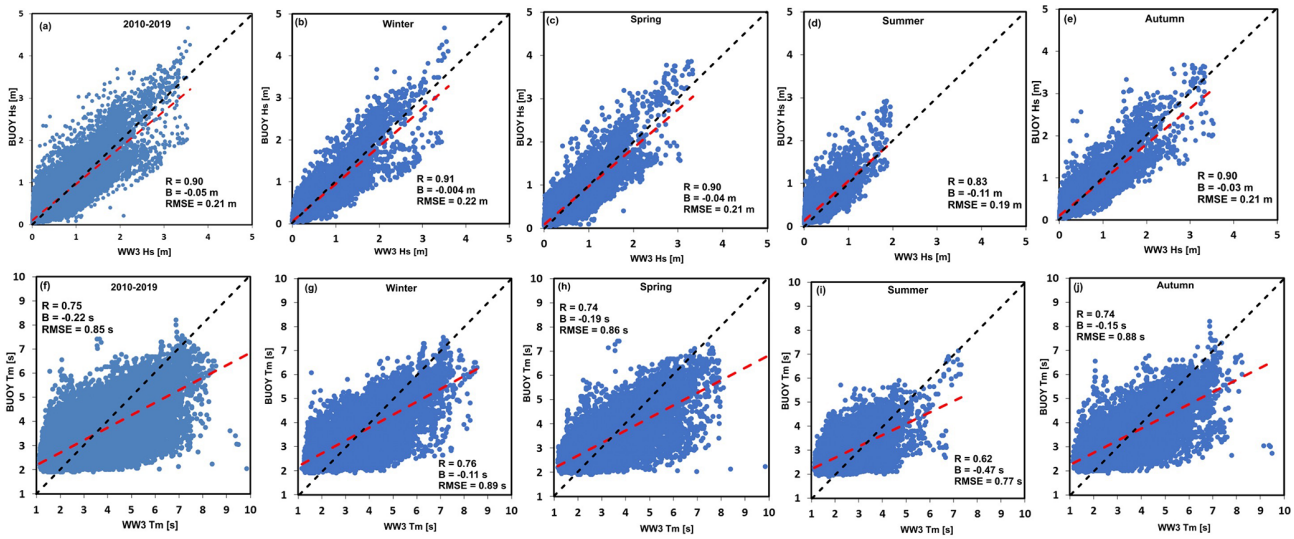

Figure 3. Observations–model scatter plot of H_s (in metres) for **(a)** 2010–2019, **(b)** winter, **(c)** spring, **(d)** summer, and **(e)** autumn (top panels) at station 6 (Cesenatico; see Fig. 1c for location). The bottom panels show scatter plots of the mean wave period (T_m in seconds) for **(f)** 2010–2019, **(g)** winter, **(h)** spring, **(i)** summer, and **(j)** autumn. The dashed black line indicates the best fit (1 : 1 slope), and the dashed red line represents the data fit. (R: correlation; B: bias; RMSE: root mean square error.)

4.1.1 Climatology of wind speed and direction

Analysis of wind speed and direction over the ER coast for the period 2010–2019 is presented in Fig. 4. The annual mean characteristics showed a very precise pattern, with the winds reaching the coast from the east-northeast. The annual mean wind speeds were of the order of 0.5–2 m s^{-1}, with a large standard deviation (SD) of 1.6–3 m s^{-1}.

The lowest wind speeds were observed during spring and summer (1.5 and 1.8 m s^{-1}), followed by autumn (2.4 m s^{-1}), with the highest wind speeds (2.9 m s^{-1}) during winter. Overall, for the winter and spring the approaching wind is easterly, related to the bora wind climatological direction. In the summer, the mean wind direction is from the southeast, owing to sirocco events. The spatial distribution of the seasonal and annual SD of wind speed from 2010–2019 is shown in Fig. 4f–j. The annual SD varies from 1.6 to 3 m s^{-1} in the entire domain (Fig. 4j), and the annual maximum is further offshore from the ER coastal belt. During the winter (Fig. 4f), the SD varies from 2.2 to 3 m s^{-1} and, in spring, from 1.2–3 m s^{-1} (Fig. 4g). While in summer and autumn, the SDs are 2.2–2.6 and 1.6–3 m s^{-1} respectively.